Cooperative Self-Assembly of Platinum(II) Acetylide Complexes

Yu-Jing Tian,[a] *E. W. Meijer,*[b] *and Feng Wang**[a,b]

[a]*Key Laboratory of Soft Matter Chemistry,*
Department of Polymer Science and Engineering,
University of Science and Technology of China,
Hefei, Anhui 230026 (P. R. China)
Fax: (+86) 551 3606 095; E-mail: drfwang@ustc.edu.cn.

[b] *Institute for Complex Molecular Systems,*
Eindhoven University of Technology,
PO Box 513, 5600 MB Eindhoven (The Netherlands).

Supporting Information

1. Materials and methods

All solvents were reagent grade, except for spectrophotometric grade methylcyclohexane and chloroform (Aldrich). 4-Iodoaniline, *N*-(3-dimethylaminopropyl)-*N′*-ethylcarbodiimide hydrochloride (EDC·HCl), 4-dimethylamino pyridine (DMAP) were reagent grade and used as received. All other chemicals were employed as purchased. 3,4,5-Trisdecyloxybenzoic acid was prepared according to a previously reported procedure.[S1]

UV/Vis and CD measurements were performed on a Jasco J-815 spectropolarimeter, for which the sensitivity, time constants and scan rates were chosen appropriately. Corresponding temperature-dependent measurements were performed with a PFD-425S/15 Peltier-type temperature controller with a temperature range of 263–323 K and adjustable temperature slope; in all cases a temperature slope of 40 $K \cdot h^{-1}$ was used. In all other measurements the temperature was set at 20 °C. In all experiments the linear dichroism was also measured, and in all cases no linear dichroism was observed. Separate UV/Vis spectra were obtained from a PerkinElmer UV/Vis spectrometer Lambda 40 at 20 °C. Cells with an optical path length of 5 mm and spectroscopic-grade solvents were employed. Solutions were prepared by weighing in the necessary amount of compound for a given concentration and transferring it to a volumetric flask. Then the flask was three-quarters filled with the spectroscopic grade solvent and put in an oscillation. Proton chemical shifts were reported in ppm downfield from tetramethylsilane (TMS). Carbon chemical shifts were reported relative to the resonance of $CDCl_3$ as internal standard. Electrospray ionization mass spectra (ESI-MS) were obtained on a Bruker Esquire 3000 plus mass spectrometer (Bruker-Franzen Analytik GmbH Breman, Germany) equipped with an ESI interface and ion trap analyzer.

*2. Synthetic routes to the compounds **1** and (S)-**2***

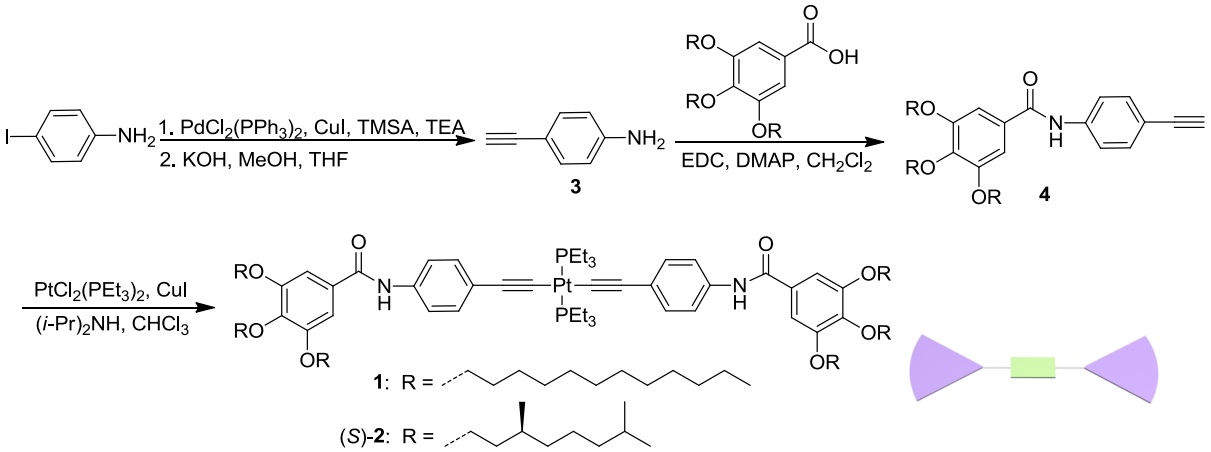

Scheme S1. Synthetic routes to the target compounds **1** and (*S*)-**2**.

*2.1. Synthesis of compound **3***

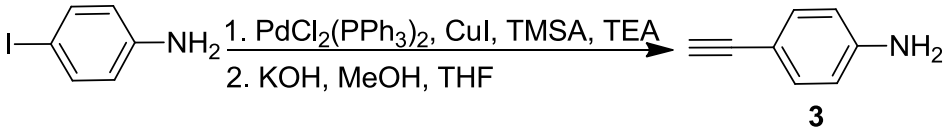

4-Iodoaniline (1.00 g, 4.56 mmol), bis(triphenylphosphine)palladium (II) dichloride (88 mg, 0.13 mmol) and CuI (22 mg, 0.12 mmol) were added to a round-bottom flask. The vessel was sealed with a rubber septum, evacuated and backfilled with nitrogen for three times. TEA (20 mL) was added *via* a syringe and the mixture was stirred for 0.5 h. Trimethylsily acetylene (0.78 mL, 5.50 mmol) was subsequently added and the reaction mixture was stirred at 40 °C for 12 h. The organic phase was extracted with water/ethyl acetate (3×), washed with brine and the solvent was removed with a rotary evaporator. The crude product was purified by flash column chromatography to afford 4-(trimethylsilylethynyl)aniline as a yellow solid (0.80 g, 93%). Next, to a stirred solution of 4-(trimethylsilylethynyl)aniline (804 mg, 4.25 mmol) in THF (5 mL), KOH (477 mg, 8.50 mmol) in methanol (6 mL) was added. After the mixture was stirred at 35 °C for 12 h, the solvent were removed. The residue was extracted with water/ethyl acetate (3×), washed with brine and the solvent was removed with a rotary evaporator. The crude product was purified by flash column chromatography (petroleum ether/ethyl acetate, 8 : 1, *v/v* as the eluent) to provide compound **3** as a pale yellow solid (449

mg, 95%).[S2] The ^{1}H NMR spectrum of compound **3** is shown in Figure S1. ^{1}H NMR (300 MHz, $CDCl_3$, room temperature) δ (ppm): 7.30 (d, 2H), 6.60 (d, 2H), 3.81 (s, 2H), 2.95 (s, 1H).

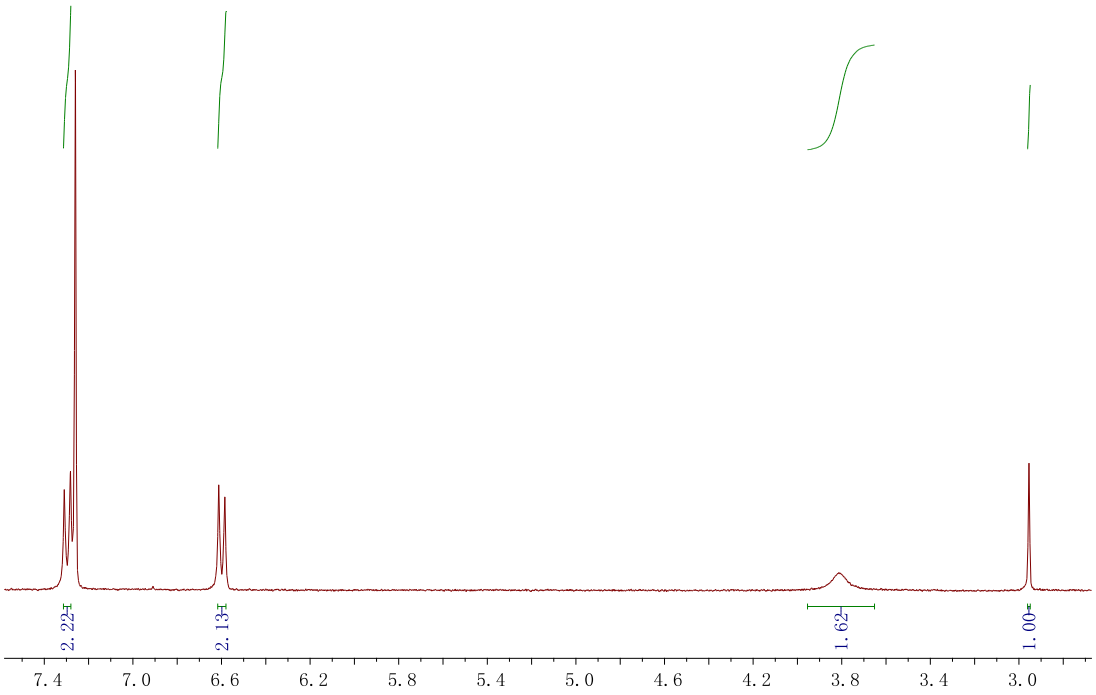

Figure S1. ^{1}H NMR spectrum (300 MHz, $CDCl_3$, room temperature) of compound **3**.

*2.2 Synthesis of compound **4a***

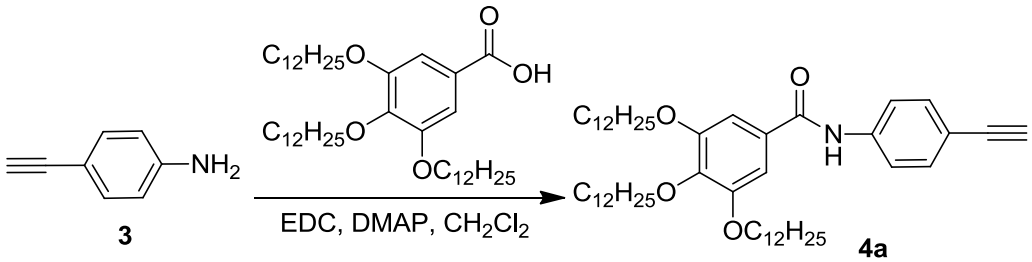

4-Aminophenylacetylene **3** (200 mg, 1.71 mmol), 3,4,5-trisdodecyloxybenzoic acid (1.38 g, 2.04 mmol), EDC·HCl (457 mg, 2.38 mmol) and DMAP (208 mg, 1.71 mmol) were dissolved in CH_2Cl_2 and the reaction mixture was stirred for 2 days at room temperature. Subsequently, the resulting mixture was extracted with water/CH_2Cl_2 (3×), washed with brine and the solvent was removed with a rotary evaporator. The residue was purified by flash column chromatograph (petroleum ether/ethyl acetate, 4 : 1, *v/v* as the eluent) to afford compound **4a**

as a white solid (1.14 g, 86%).[S3] The ^{1}H NMR spectrum of compound **4a** is shown in Figure S2. ^{1}H NMR (300 MHz, $CDCl_3$, room temperature) δ (ppm): 7.76 (s, 1H), 7.61 (d, 2H), 7.49 (d, 2H), 7.03 (s, 2H), 4.02 (m, 6H), 3.06 (s, 1H), 1.88–1.68 (m, 6H), 1.50–1.25 (m, 54H), 0.88 (t, 9H).

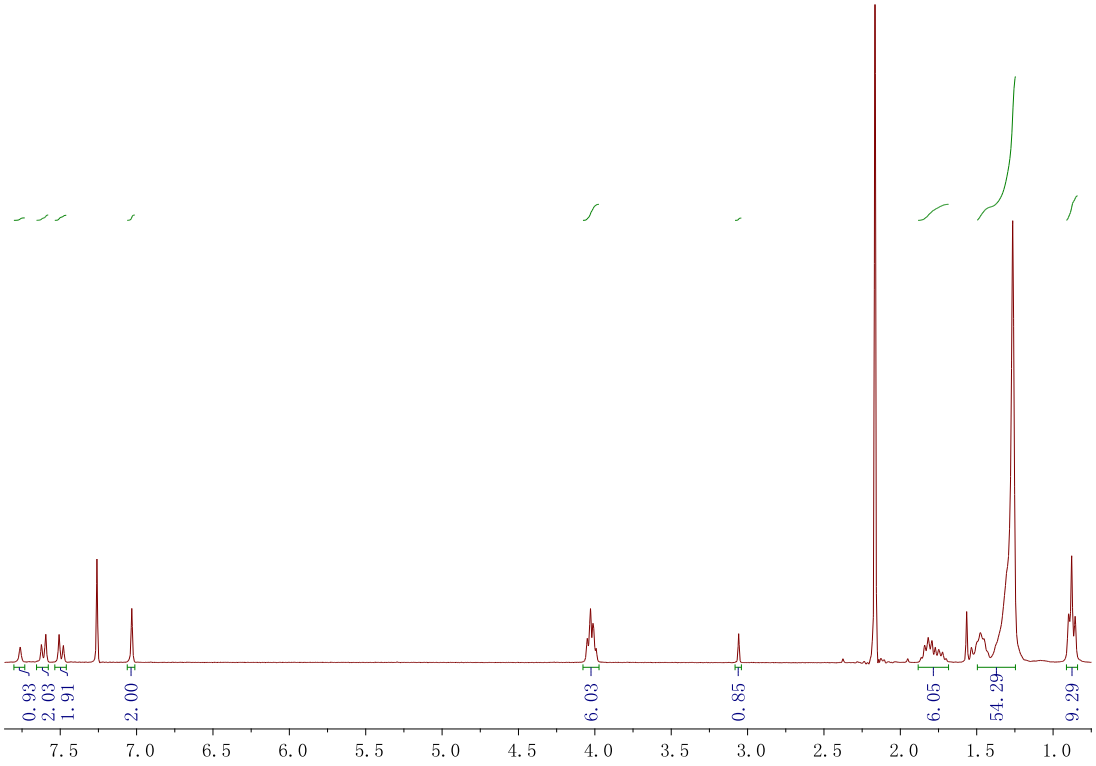

Figure S2. ^{1}H NMR spectrum (300 MHz, $CDCl_3$, room temperature) of compound **4a**.

*2.3 Synthesis of compound (S)-**4b***

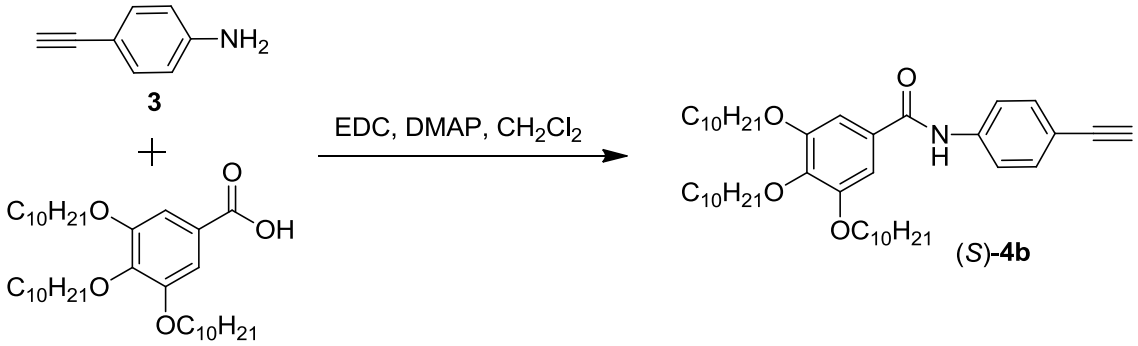

A mixture of compound **3** (120 mg, 1.03 mmol), (*S*)-3,4,5-trisdecyloxybenzoic acid (400 mg, 0.68 mmol), EDC·HCl (250 mg, 1.30 mmol) and DMAP (120 mg, 0.98 mmol) was stirred for 3 days at room temperature. Subsequently, the resulting mixture was extracted with water/CH_2Cl_2 (3×), washed with brine and the solvent was removed with a rotary evaporator.

The residue was purified by flash column chromatograph (petroleum ether/THF, 60 : 1, *v/v* as the eluent) to afford compound (*S*)-**4b** as a white solid (375 mg, 80%). The ^{1}H NMR spectrum of compound (*S*)-**4b** is shown in Figure S3. ^{1}H NMR (300 MHz, $CDCl_3$, room temperature) δ (ppm): 7.71 (s, 1H), 7.61 (d, 2H), 7.50 (d, 2H), 7.04 (s, 2H), 4.06 (m, 6H), 3.07 (s, 1H), 1.91 – 1.80 (m, 3H), 1.76 – 1.58 (m, 6H), 1.50 (m, 3H), 1.36 – 1.13 (m, 18H), 0.97 – 0.91 (m, 9H), 0.87 (d, 18H). The ^{13}C NMR spectrum of compound (*S*)-**4b** is shown in Figure S4. ^{13}C NMR (75 MHz, $CDCl_3$, room temperature) δ (ppm): 164.6, 152.3, 140.7, 137.5, 132.0, 128.6, 118.7, 116.9, 104.8, 82.4, 70.8, 66.8, 38.4, 36.5, 35.4, 29.9, 28.8, 27.0, 23.7, 21.7, 18.6. ESI–MS m/z: $[M + H]^+$ $C_{45}H_{72}NO_4$, 690.569.

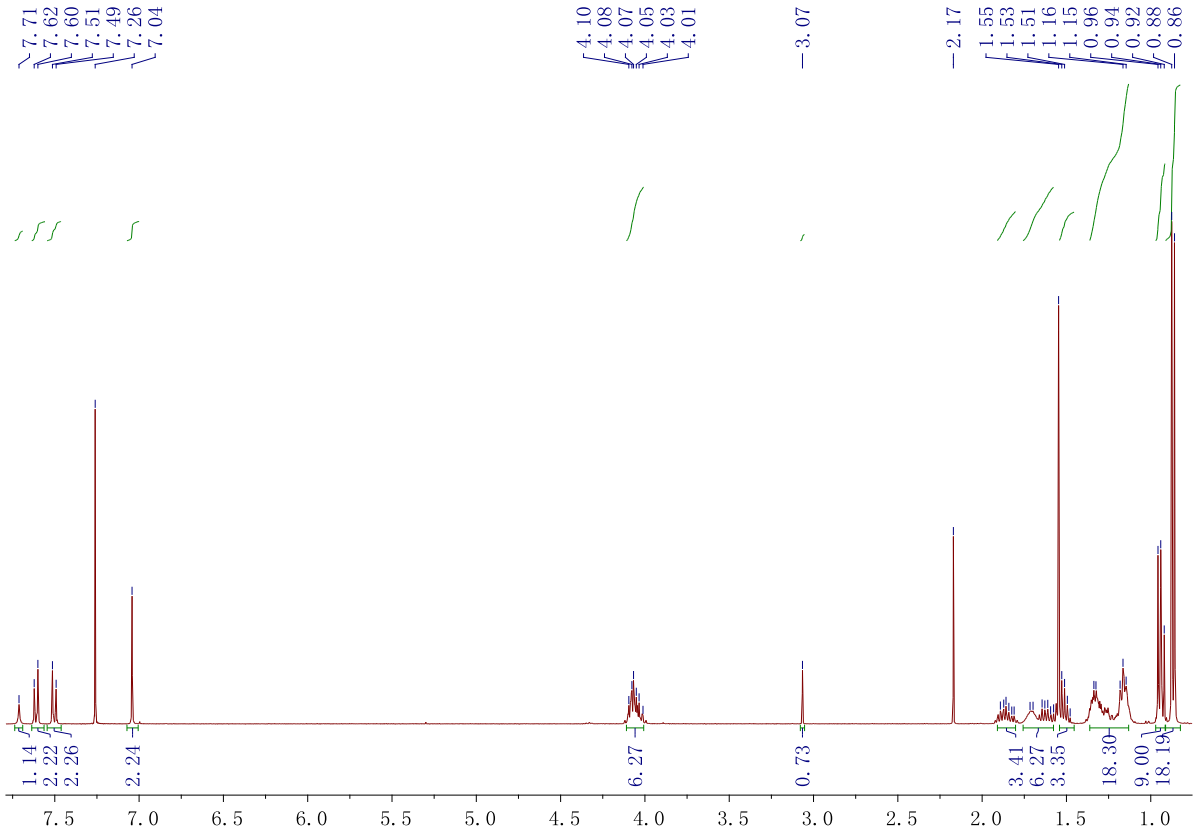

Figure S3. ^{1}H NMR spectrum (300 MHz, $CDCl_3$, room temperature) of compound (*S*)-**4b**.

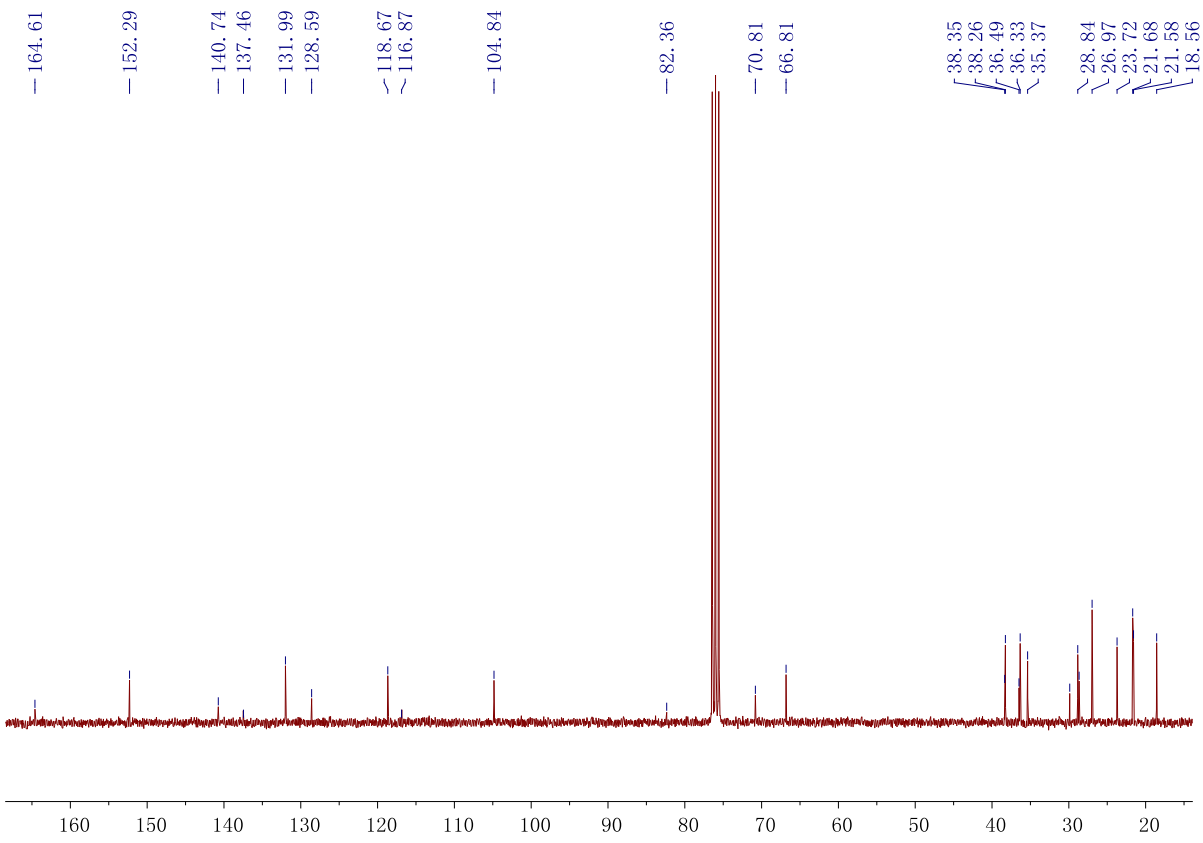

Figure S4. ^{13}C NMR spectrum (75 MHz, $CDCl_3$, room temperature) of compound (*S*)-**4b**.

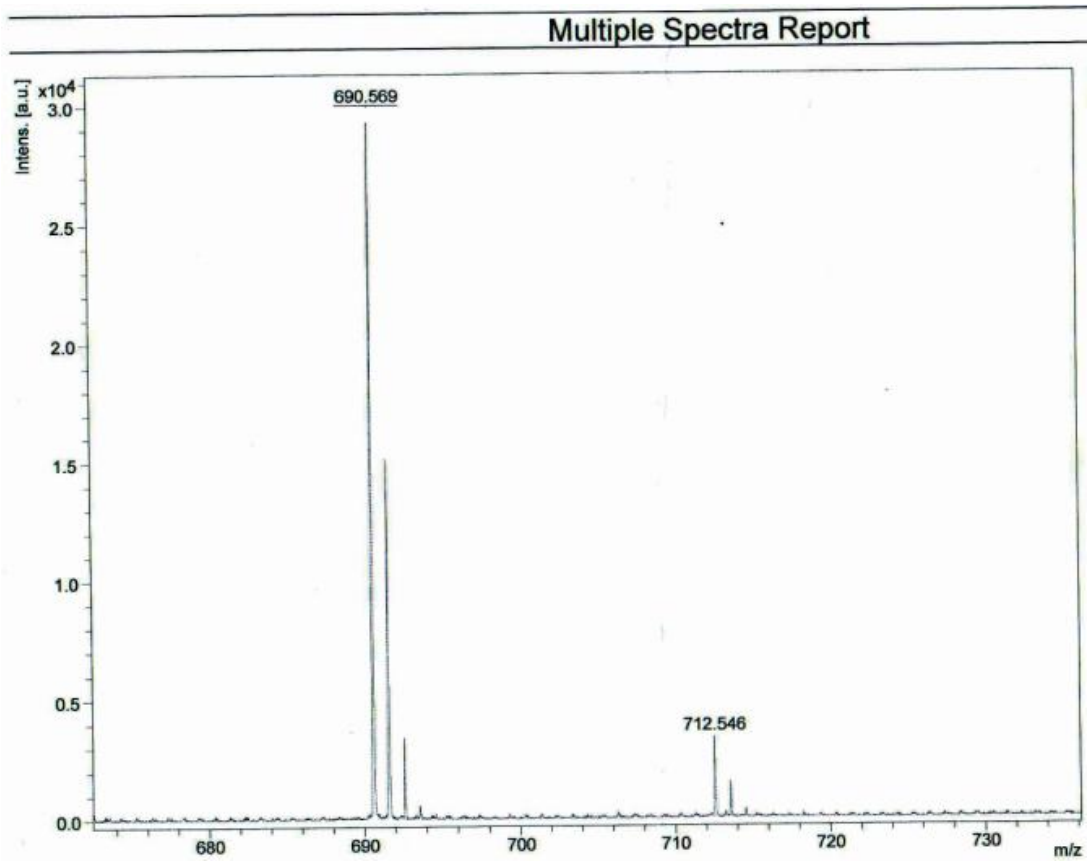

Figure S5. Electrospray ionization mass spectrum of compound (*S*)-**4b**.

*2.4 Synthesis of compound **1***

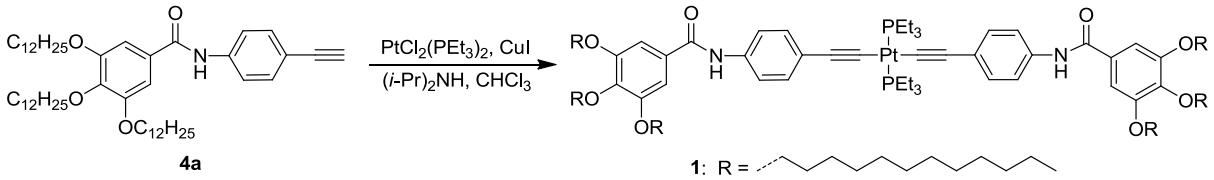

Compounds **4a** (309 mg, 0.40 mmol), *trans*-$Pt(PEt_3)_2Cl_2$ (100 mg, 0.20 mmol), CuI (4 mg, 0.02 mmol) in $CHCl_3$/(*i*-Pr)$_2$NH (50 mL, 1 : 1, *v/v*) were stirred at 40 °C for 3 days. The solvents were then removed and the resulting mixture was extracted with water/CH_2Cl_2 (3×), washed with brine and the solvent was removed with a rotary evaporator. The residue was purified by flash column chromatograph (petroleum ether/dichloromethane/THF, 20 : 5 : 1, *v/v/v* as the eluent) to afford compound **1** as a yellow solid (355 mg, 90%). M.p.: 130.3–132.0 °C. The ^{1}H NMR spectrum of compound **1** is shown in Figure S6. ^{1}H NMR (300 MHz, $CDCl_3$, room temperature) δ (ppm): 7.63 (s, 2H), 7.47 (d, 4H), 7.27 (d, 4H), 7.03 (s, 4H), 4.07–3.97 (m, 12H), 2.24–2.15 (m, 12H), 1.85–1.76 (m, 12H), 1.51–1.03 (m, 126H), 0.88 (t, 18H). The ^{13}C NMR spectrum of compound **1** is shown in Figure S7. ^{13}C NMR (100 MHz, $CDCl_3$, room temperature) δ (ppm): 165.3, 153.2, 141.5, 135.0, 131.5, 130.1, 119.8, 105.8, 73.5, 69.5, 31.9, 30.3, 29.8, 29.7, 29.6, 29.4, 26.1, 22.7, 16.6, 16.4, 16.2, 14.1, 8.4. The ^{31}P NMR spectrum of compound **1** is shown in Figure S8. ^{31}P NMR (162 MHz, $CDCl_3$, room temperature) δ (ppm): 10.94 (t, J = 2932 Hz). ESI–MS m/z: $[M + H]^+$ $C_{114}H_{195}N_2O_8P_2Pt$, 1977.415.

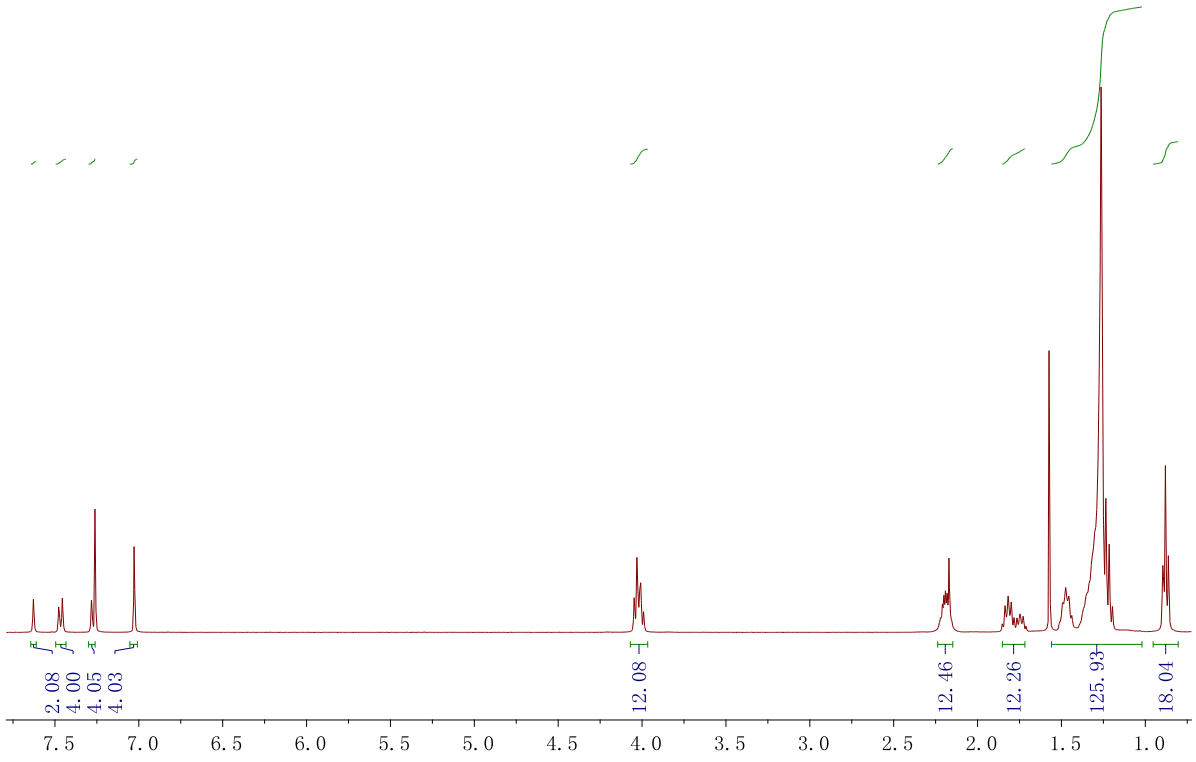

Figure S6. ^{1}H NMR spectrum (400 MHz, $CDCl_3$, room temperature) of compound **1**.

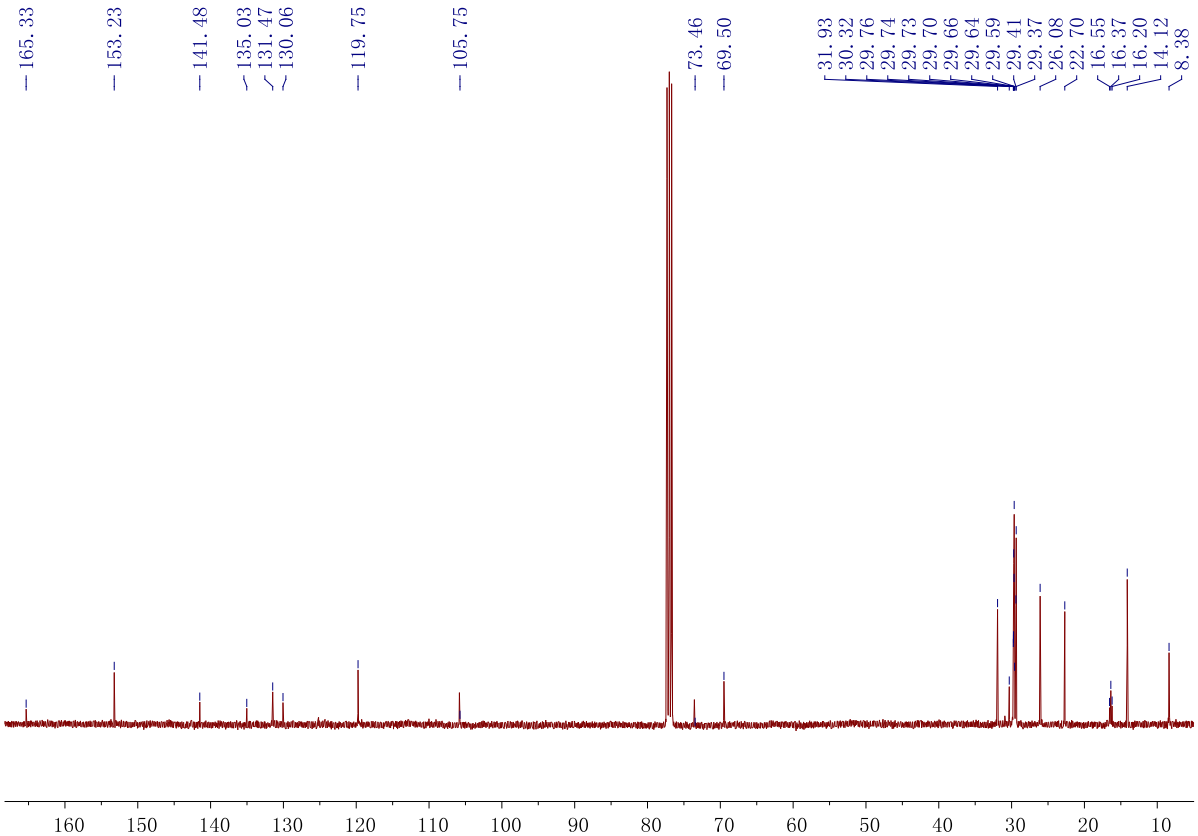

Figure S7. ^{13}C NMR spectrum (100 MHz, $CDCl_3$, room temperature) of compound **1**.

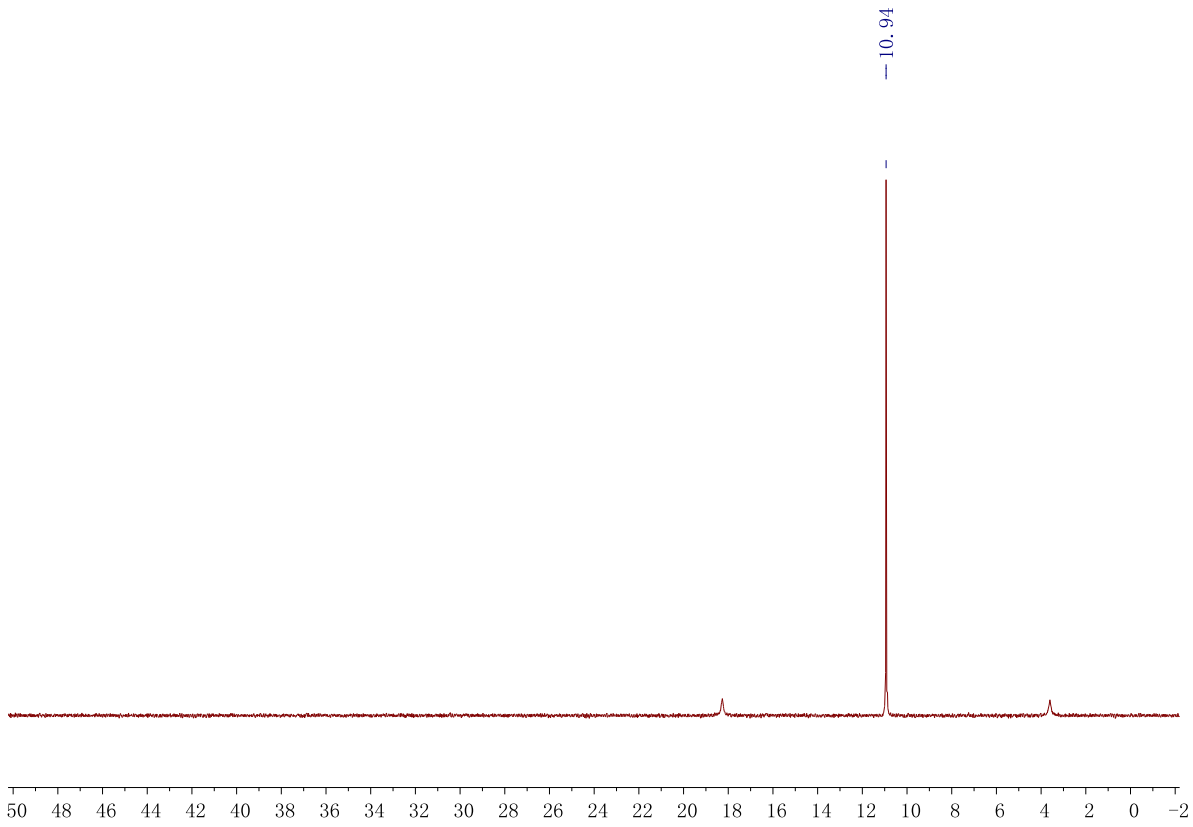

Figure S8. ^{31}P NMR spectrum (162 MHz, $CDCl_3$, room temperature) of compound **1**.

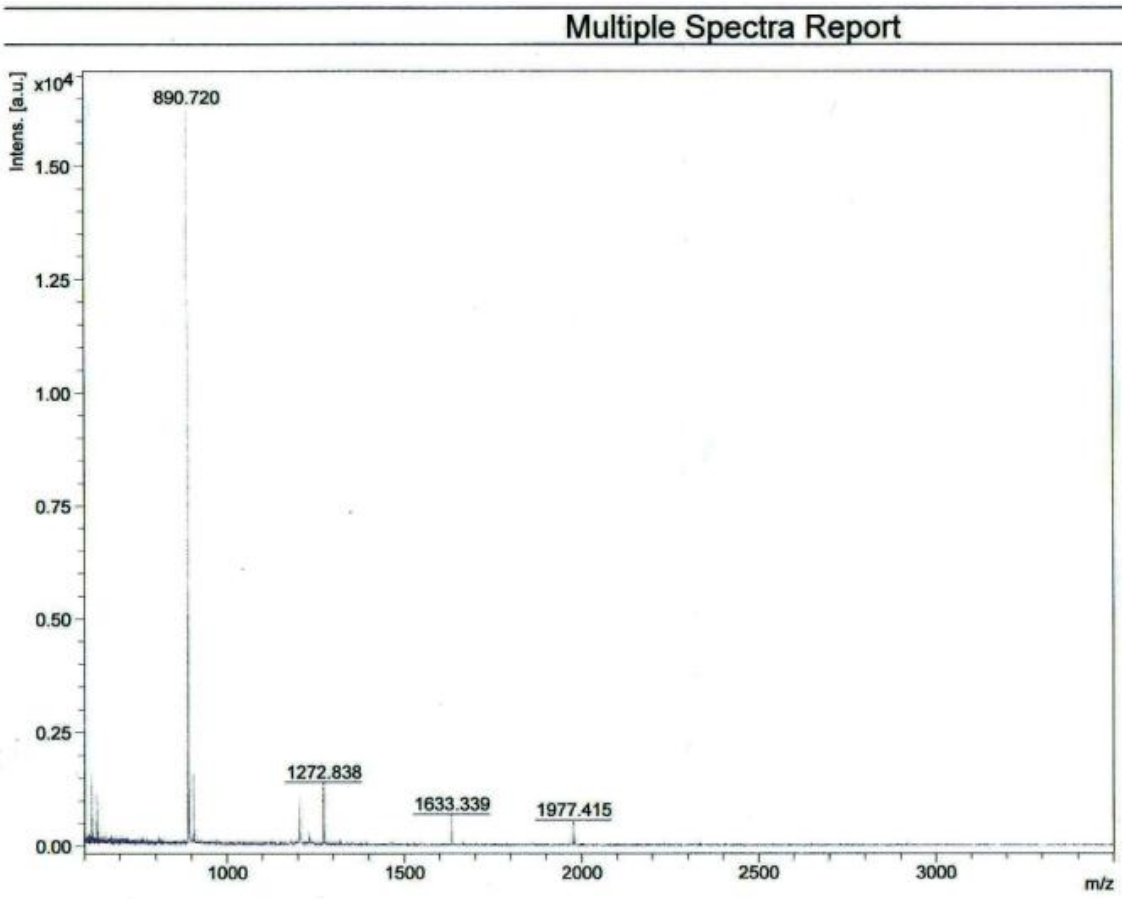

Figure S9. Electrospray ionization mass spectrum of compound **1**.

*2.5 Synthesis of compound (S)-**2***

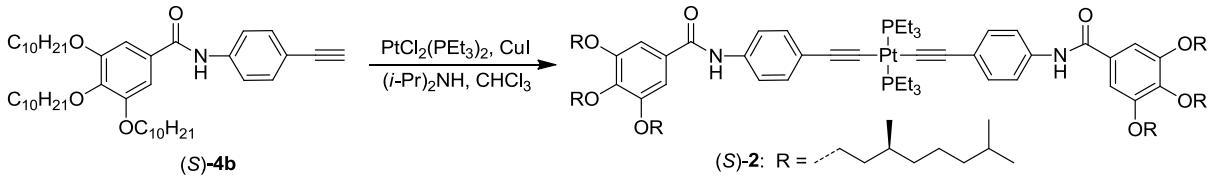

Compounds (*S*)-**4b** (375 mg, 0.54 mmol), *trans*-$Pt(PEt_3)_2Cl_2$ (140 mg, 0.28 mmol), CuI (6 mg, 0.03 mmol) in $CHCl_3$/(*i*-Pr)$_2$NH (50 mL, 1 : 1, *v/v*) were stirred at 40 °C for 3 days. The solvents were then removed and the resulting mixture was extracted with water/CH_2Cl_2 (3×), washed with brine and the solvent was removed with a rotary evaporator. The residue was purified by flash column chromatograph (petroleum ether/dichloromethane/THF, 20 : 5 : 1, *v/v/v* as the eluent) to afford compound **(*S*)-2** as a yellow solid (452 mg, 89%). M.p.: 160.8–162.0 °C. The ^{1}H NMR spectrum of compound (*S*)-**2** is shown in Figure S10. ^{1}H NMR (400 MHz, $CDCl_3$, room temperature) δ (ppm): 7.63 (s, 2H), 7.47 (d, 4H), 7.29 (d, 4H), 7.04 (s, 4H), 4.06 (m, 12H), 2.24–2.17 (m, 12H), 1.91–1.81 (m, 6H), 1.76–1.55 (m, 12H), 1.52 (m, 6H), 1.40–1.27 (m, 18H), 1.26–1.21 (m, 18H), 1.20–1.11 (m, 18H), 0.94 (m,18H), 0.87 (d, 36H). The ^{13}C NMR spectrum of compound (*S*)-**2** is shown in Figure S11. ^{13}C NMR (100 MHz, $CDCl_3$, room temperature) δ (ppm): 165.3, 153.2, 141.4, 135.0, 131.5, 130.0, 119.8, 105.8, 71.8, 67.8, 39.4, 39.3, 37.5, 37.3, 36.4, 29.9, 29.7, 28.0, 24.7, 22.7, 22.6, 19.6, 16.5, 16.4, 16.2, 8.4. The ^{31}P NMR spectrum of compound (*S*)-**2** is shown in Figure S12. ^{31}P NMR (162 MHz, $CDCl_3$, room temperature) δ (ppm): 10.95 (t, J = 2936 Hz). ESI–MS m/z: $[M + H]^+$ $C_{102}H_{171}N_2O_8P_2Pt$, 1809.196.

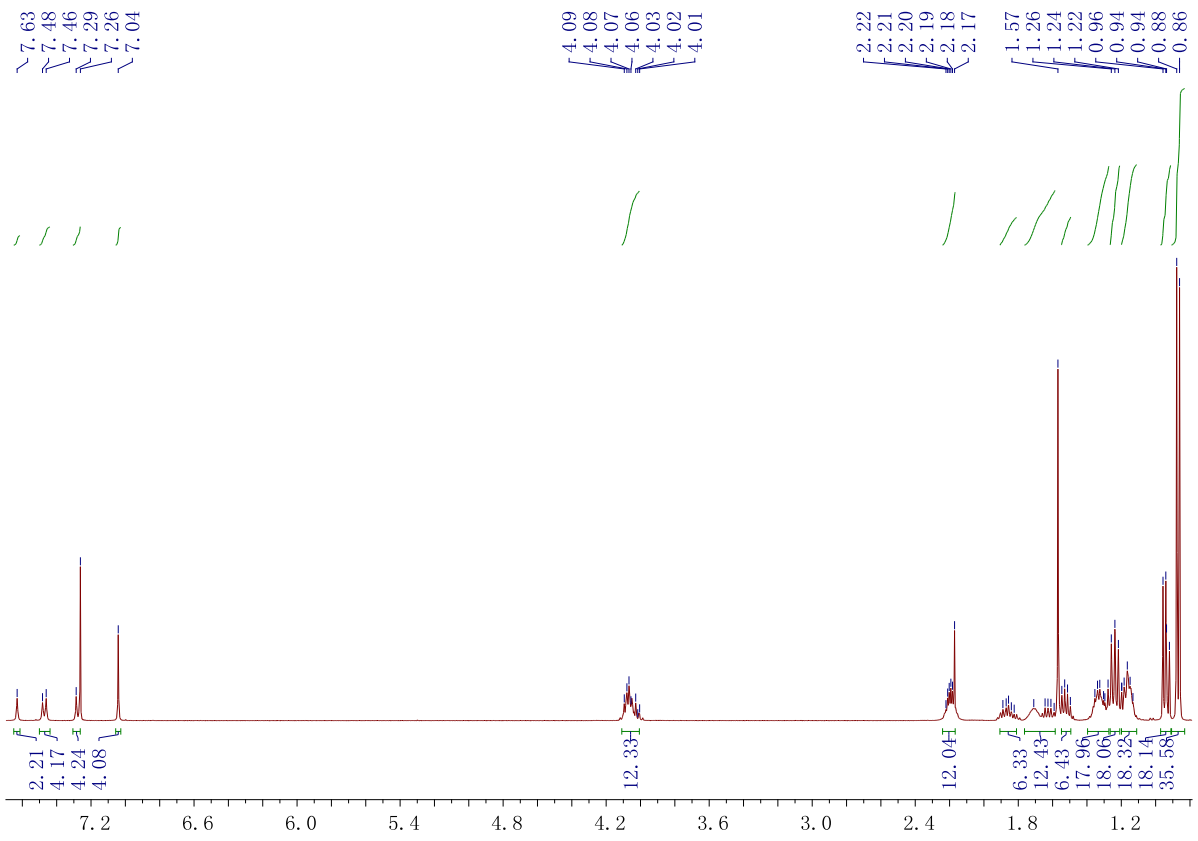

Figure S10. ^{1}H NMR spectrum (400 MHz, $CDCl_3$, room temperature) of compound (*S*)-**2**.

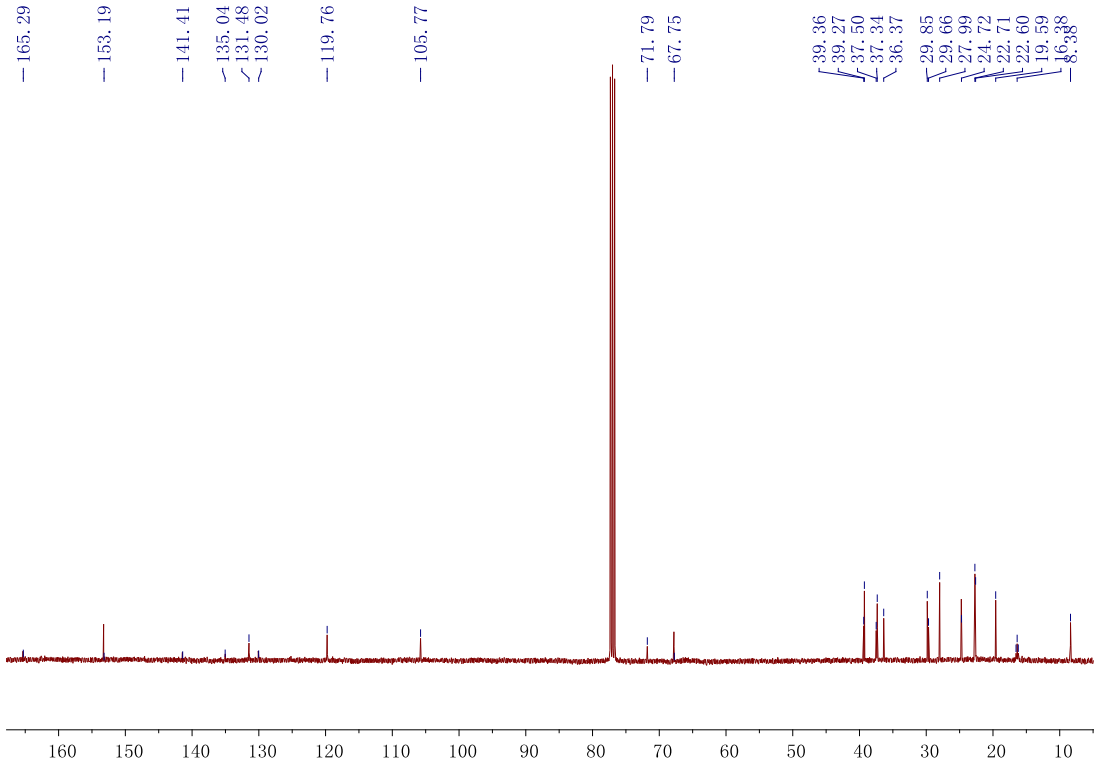

Figure S11. ^{13}C NMR spectrum (100 MHz, $CDCl_3$, room temperature) of compound (*S*)-**2**.

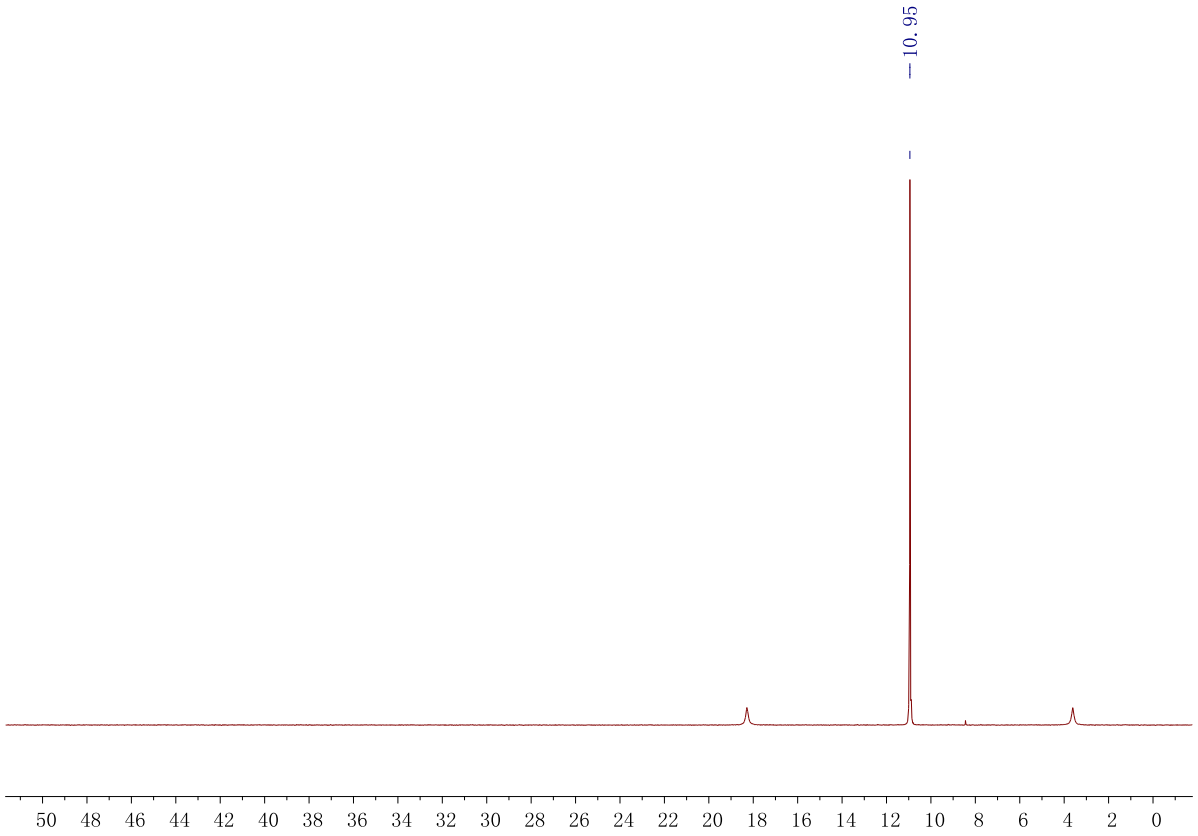

Figure S12. ^{31}P NMR spectrum (162 MHz, $CDCl_3$, room temperature) of compound (*S*)-**2**.

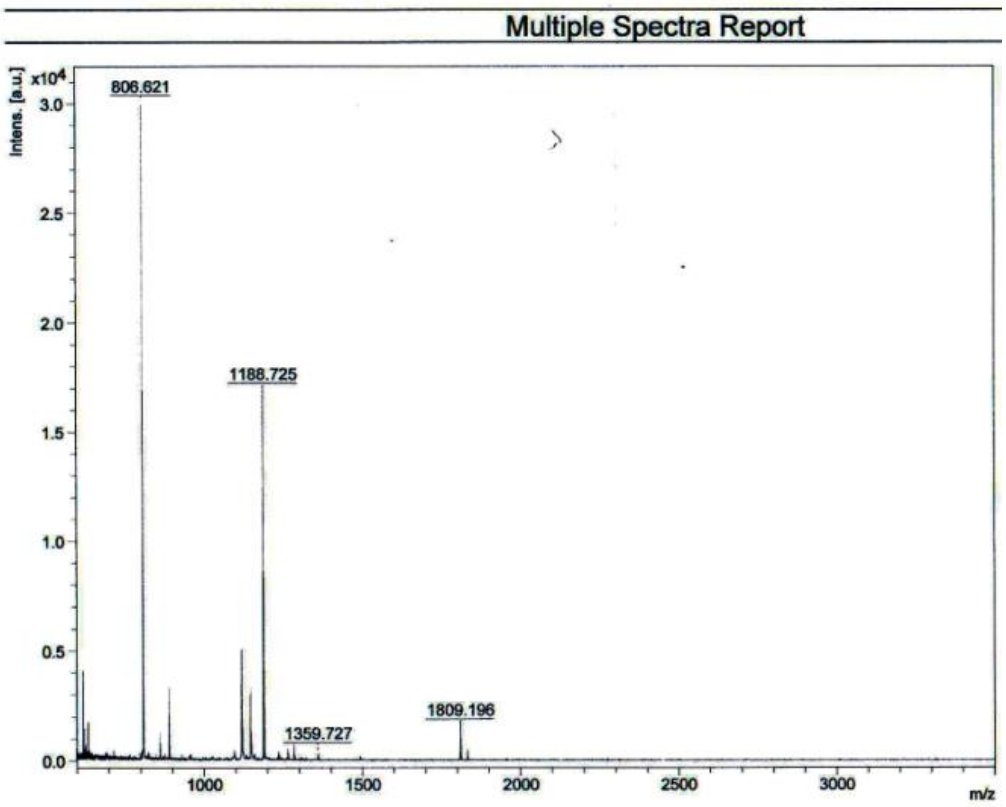

Figure S13. Electrospray ionization mass spectrum of compound (*S*)-**2**.

*3. Differential scanning calorimetry measurements of compound **1** and (S)-**2***

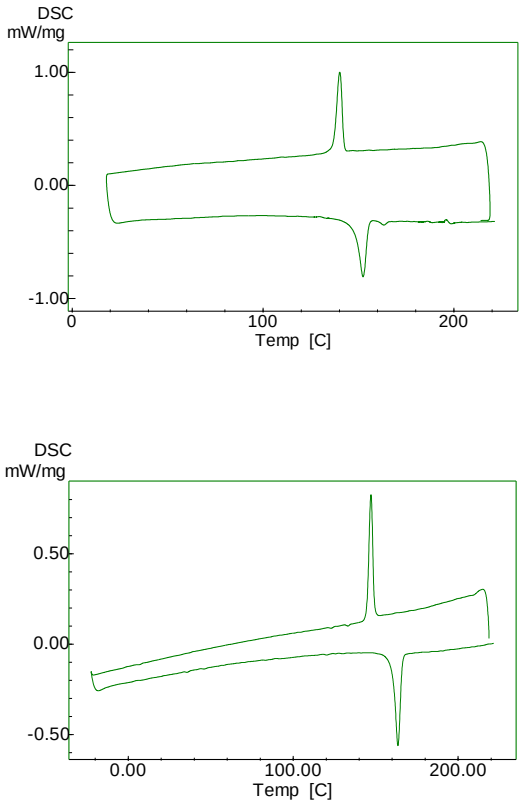

Figure S14. DSC measurements of compounds **1** and (*S*)-**2**. The first cooling and second heating run exhibit the liquid crystalline phase for both compounds.

*4. UV-Vis spectra of compound **1** and (S)-**2***

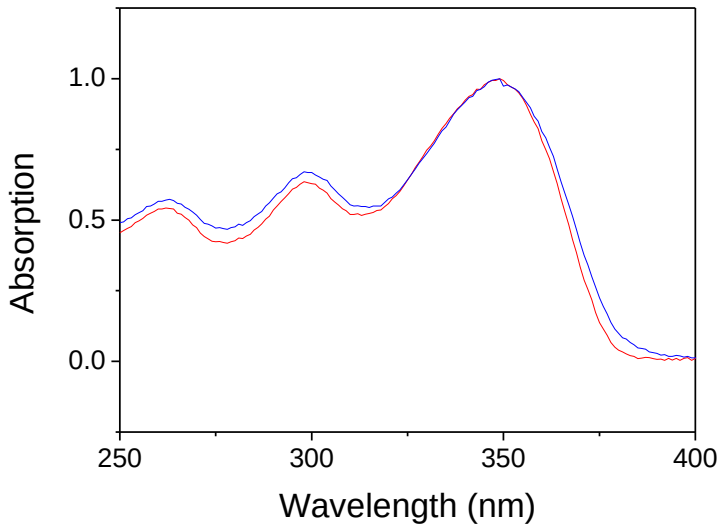

Figure S15. Absorption spectra of **1** (red line) and (*S*)-**2** (blue line) in MCH solution (c = 5×10^{-5} M, 2 mm cuvette, 20 ºC). The essentially identical UV-Vis absorption patterns are observed for both compounds, suggesting that the chain length of the alkoxy groups does not have any significant effect on the aggregate behavior.

*5. Fluorescent spectra of compound **1** in the gel and film state*

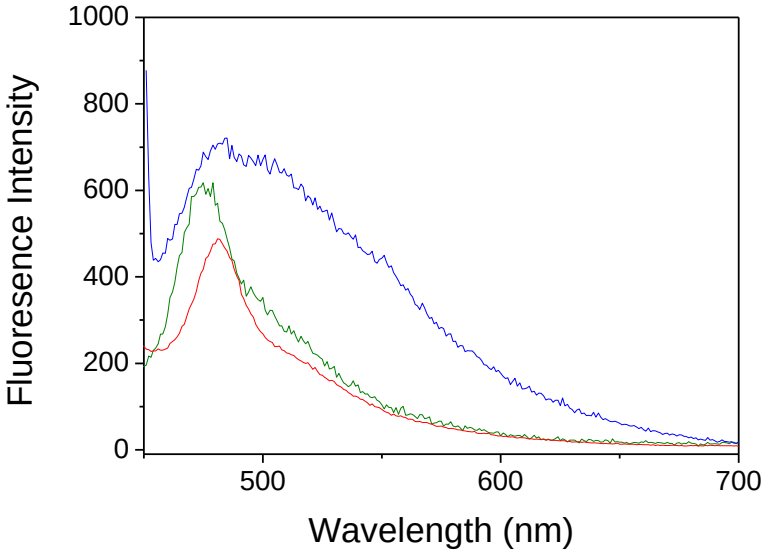

Figure S16. Fluorescence emission spectra of **1** in gel state (blue line, λ_{ex} = 435 nm) and in the doped poly(methyl methacrylate) (PMMA) films (green line, 0.5% (quality ratio of **1** in PMMA); red line, 25% (quality ratio of **1** in PMMA); λ_{ex} = 365 nm). The non-radiative decay process was significantly suppressed in the gel or film state due to the presence of intermolecular stacking and thereby inhibition of intramolecular rotation.

*6. Temperature dependent ^{1}H NMR spectra of compound **1** in d_{12}-cyclohexane*

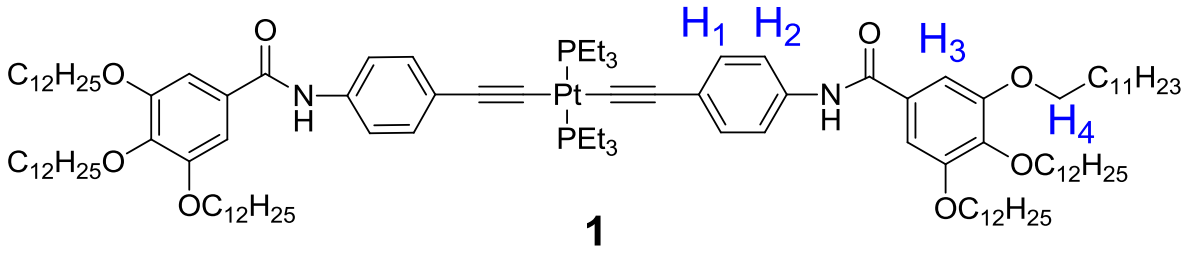

1

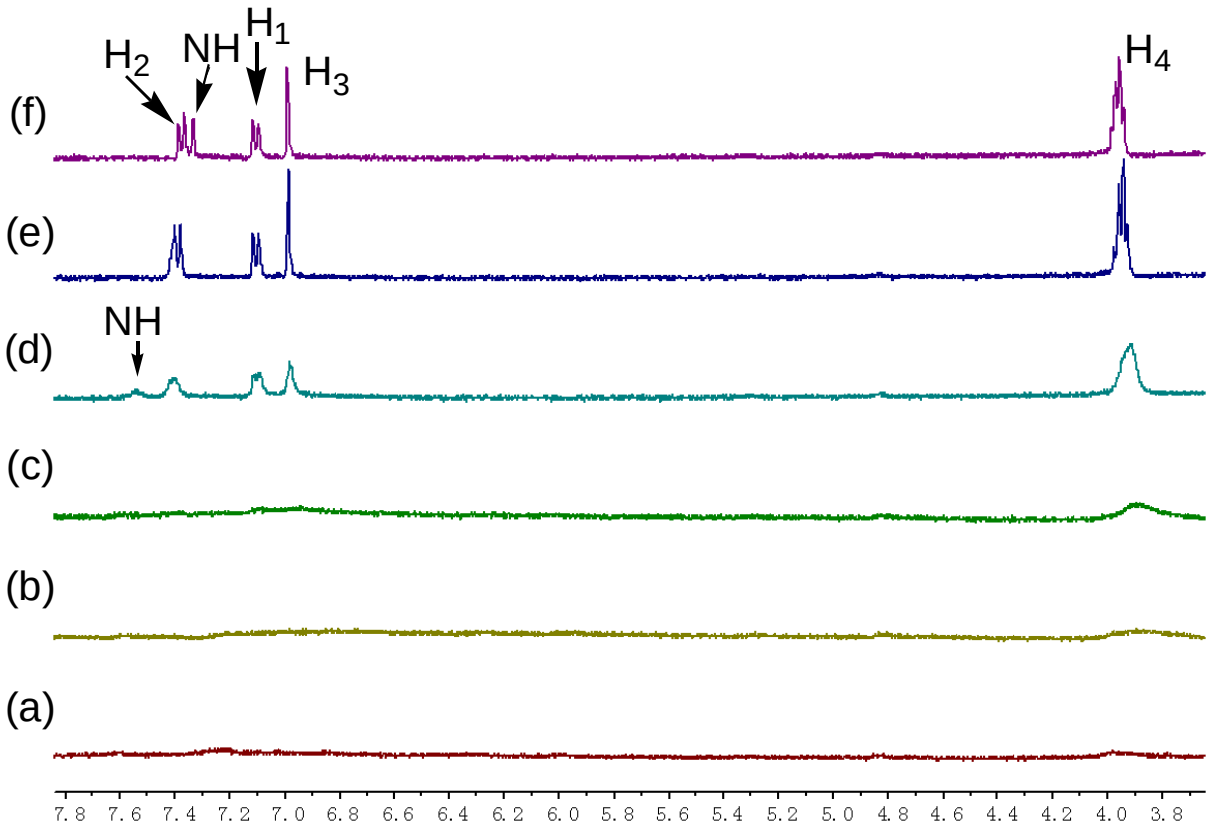

Figure S17. Partial temperature-dependent ^{1}H NMR spectra of **1** in d_{12}-cyclohexane at different temperatures: (a) 20 ºC, (b) 30 ºC, (c) 40 ºC, (d) 50 ºC, (e) 60 ºC, (f) 70 ºC. **(**all measurements: concentration = 2 mM)

Self-assembly of compound **1** was probed by temperature-dependent ^{1}H NMR spectra at the monomer concentration of 2 mM. We choose non-polar d_{12}-cyclohexane as the solvent, in which both π–π stacking and hydrogen-bonding interaction are more favorable than those in chloroform. As shown in Figure S17, the aromatic protons became significantly broad below 40 ºC, suggesting strong tendency to form high-molecular-weight aggregates. Warming to 50 ºC resulted in sharpening of the signals. In addition, the amide protons were significantly upfield shifted upon increasing the temperature, suggesting hydrogen-bonding interactions are also involved in the surpamolecular polymerization process.

*7. Concentration dependent ^{1}H NMR spectra of compound **1** in d-chloroform*

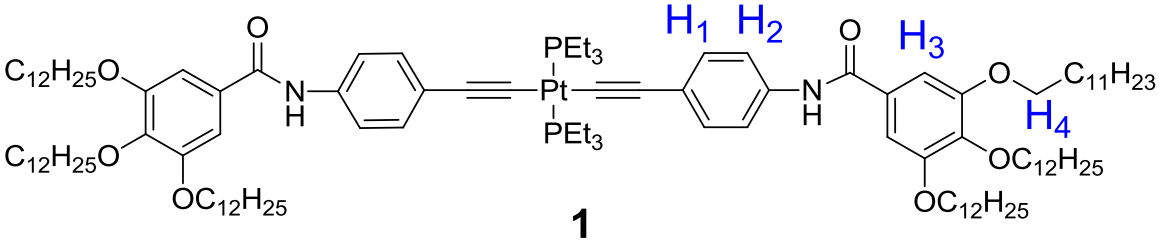

1

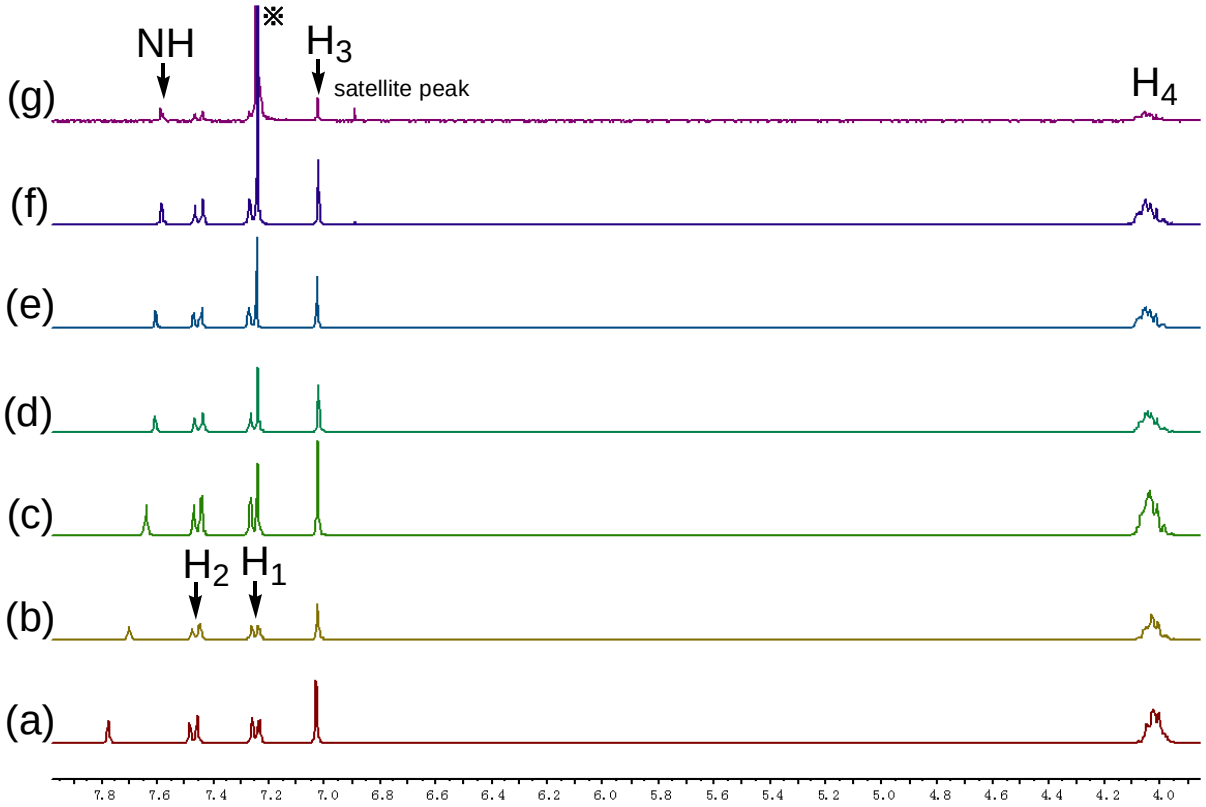

Figure S18. Partial concentration-dependent ^{1}H NMR spectra of **1** in *d*-chloroform at different concentrations: (a) 64.6, (b) 40.4, (c) 23.1, (d) 15.4, (e) 7.70, (f) 1.54, (g) 0.15 mM (all measurements: T = 25 ºC).

Self-assembly of compound **1** was also investigated by concentration-dependent ^{1}H NMR measurements in $CDCl_3$ (Figure S18). Chloroform is known to be benign for rigid π-conjugated systems. In the concentration range of 0.15–64.6 mM, significant downfield shifts were observed for the amide protons upon increasing the concentration, indicating that hydrogen bonding is a crucial driving force for the self-assembly process. No significant shifts were observed of most of the peaks corresponding to the aromatic protons, suggesting π–π stacking interaction is restricted in the polar environment.

*8. CD/UV-Vis cooling curves of (S)-**2***

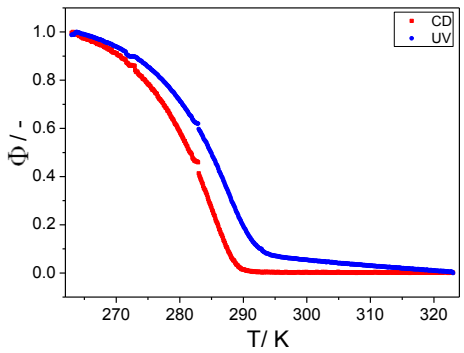

Figure S19. Net helicity Φ derived from CD and UV signals as a function of temperature for compound (*S*)-**2** in MCH, λ = 373 nm. The UV cooling curve exhibits the higher onset temperature than that of CD cooling curve, indicating small and disordered oligomers are present in the nucleation stage before the elongation into stable one-dimensional aggregates.

9. Fitting of the CD cooling curves of (S)-2

The temperature-dependent CD absorption data were normalized by fitting the increase in CD effect upon lowering the temperature with the following equations:

$$CD(T) = CD_{SAT}[1 - exp(\frac{-h_e}{RT_e^2} \times (T - T_e)]$$

Where CD_{SAT} is the limiting CD absorption at low temperature, h_e is the enthalpy release upon elongation, T_e is the elongation temperature, T is the temperature and R is gas constant. The temperature-dependent CD data were then normalized by dividing the CD value by CD_{SAT} (yielding φ(T) = CD(T)/CD_{SAT} as the dimensionless *y*-axis), and by dividing the temperature by T_e (yielding the dimensionless temperature T/T_e on the *x*-axis). The details of this procedure are described in reference S4.

For the compound (*S*)-**2** at 5×10^{-5} M, the normalized CD cooling curve fits very well with the model over the whole temperature range, for which the enthalpy release h_e value is –68 kJ mol^{-1} while the elongation temperature T_e value is 288 K (Figure S20c). The quantitative K_a value (the equilibrium constant of the nucleation step) could also be determined to be 3.8×10^{-4}, which reflects a moderately cooperative degree for the current system. The fitting results were further validated by performing the CD cooling curves at three different concentrations (Figure S20a–c), which exhibit concentration independent h_e and K_a values (Table S1). On the other hand, T_e value gradually increased at higher monomer concentration, suggesting the earlier formation of columnar aggregates.

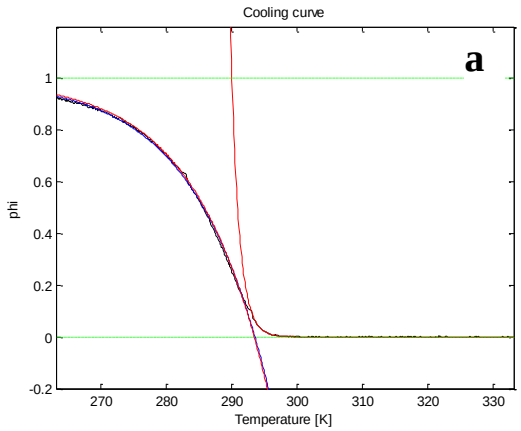

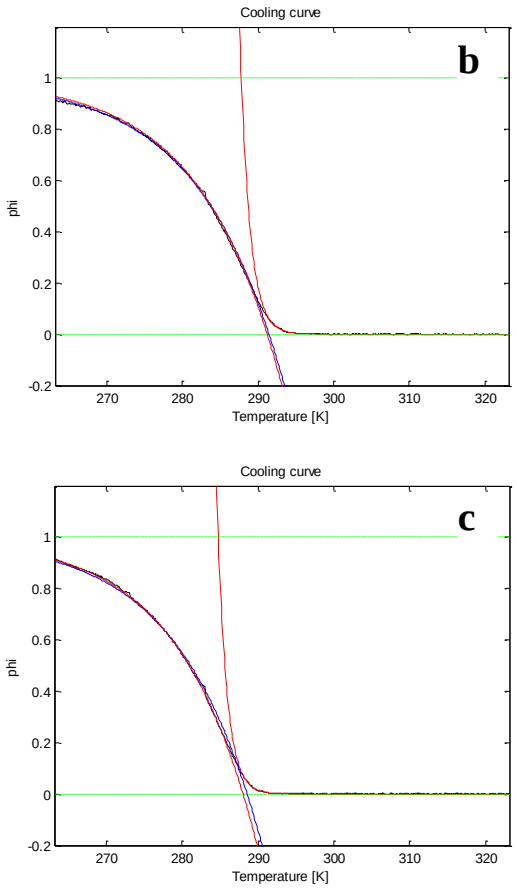

Figure S20. Net helicity Φ as a function of temperature for compound (*S*)-**2** in MCH probed at λ = 373 nm at three different concentrations: (a) 1×10^{-4} M; (b) 7.5×10^{-5} M; (c) 5×10^{-5} M. The net helicity **Φ** is defined as the difference between the fraction of M- and P-type helical aggregates ([P]–[M])/([P]+[M])) and obtained by dividing the CD effect by the maximal attainable CD effect.

10. Chiral amplification studies

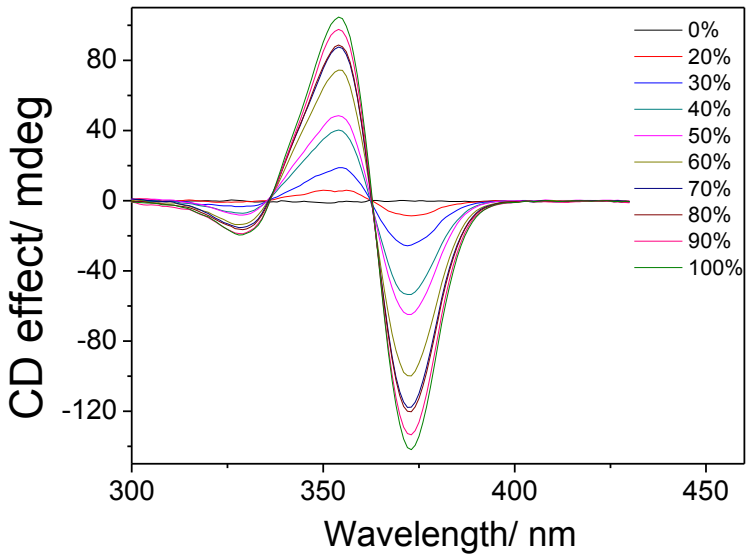

Figure S21. Sergeant-and-soldiers experiments of achiral **1** and chiral (*S*)-**2** coassemblies in

MCH solution (The percentage values in the legend refer to the proportion of *(S)*-**2** in the mixture; T = 283 K, $c = 5 \times 10^{-4}$ M, 1 mm cuvette).

References:

S1. Ghosh, S.; Li, X. Q.; Stepanenko, V.; Wurthner, F.; *Chem. Eur. J.* **2008**, *14*, 11343–11357.

S2. Li, Z. X.; Zhao, W. Y.; Zhang, Y. N.; Zhang, L. F.; Yu, M. M.; Liu, J. X.; Zhang, H. Y. *Tetrahedron*. **2011**, *67*, 7095–7100.

S3. Xu., X.-D.; Zhang, J.; Chen, L.-J.; Zhao, X.-L.; Wang, D.-X.; Yang, H.-B. *Chem. Eur. J.* **2012**, *18*, 1659–1667.

S4. Jonkheijm, P.; van der Schoot, P.; Schenning, A. P. J. H.; Meijer, E. W. *Science* **2006**, *313*, 80–83.